AIAA JOURNAL
Vol. 43, No. 12, December 2005

Predictive Elastothermodynamic Damping in Finite Element Models by Using a Perturbation Formulation

Mark J. Silver* and Lee D. Peterson†
University of Colorado, Boulder, Colorado 80309-0429
and
R. Scott Erwin‡
U.S. Air Force Research Laboratory, Kirtland Air Force Base, New Mexico 87117-5776

A method is presented by which elastothermodynamic damping can be included in finite element formulations for design analysis. In this method, elastothermodynamic damping theory is combined with a perturbation method previously developed for viscoelastic modeling. A key aspect of this approach is that it projects elastothermodynamic damping onto the undamped mode shapes of the structure. A finite element formulation is developed and presented for beams in both bending and extension. The finite element formulation creates nonsparse, nonsymmetric damping and stiffness matrices. Results with this method for various cases are discussed. After validation against the classic Zener model damping prediction, the method is applied to the analysis of damping in a three-dimensional truss. The results show that elastothermodynamic damping is higher for modes with a larger portion of their strain energy due to local member bending rather than extension. Through examples it is shown that to maximize elastothermodynamic damping in a truss, both the member cross section and the truss mode shapes must be considered.

Nomenclature

A = cross-section area of beam
B_{ij} = strain-displacement matrix
c_E = specific heat at constant deformation
D = damping terms in preassembly frequency-based stiffness matrix; subscripts L = longitudinal, T = transverse
d = thickness of a beam
$f_{,mm}$ = spatial derivative of f
$(f)^T$ = transpose of the vector or matrix f
$\tilde{f}(s)$ = laplace transform of the function $f(t)$
$\dot{f}$ = first derivative of f with respect to time
$\ddot{f}$ = second derivative of f with respect to time
I = beam area moment of inertia
i = imaginary number constant
K = complete stiffness matrix
K^e = elastic stiffness matrix
k = thermal conductivity
L = beam element length
M = mass matrix
M_R = relaxed elastic modulus
$Q(t)$ = forcing function
S_j = component j of time-varying spatial function
s = Laplace transform variable
T = temperature at deformed state
T_j = time-varying temperature function in direction j
T_0 = temperature of stress-free reference state
U^n = strain energy in mode n
u_{x1} = x-displacement degree of freedom of node 1 in the two-node beam element
V_{ijmn} = small viscoelastic relaxation tensor
x_i = spatial expansion variable
z_n = nth dual vector
α = linear thermal expansion coefficient
ΔC = damping matrix
ΔK = supplemental stiffness matrix
ΔK^t = time-varying stiffness matrix
ΔK^* = frequency-based stiffness matrix
$\Delta \tilde{K}^*$ = elemental, frequency-based stiffness matrix
δ_{ij} = Kronecker delta
ε = strain in a standard linear solid
ε_{ij} = strain tensor
ζ = critical damping fraction
η^n = fraction of strain energy due to bending in mode n
θ_{x1} = x rotational degree of freedom of node 1 in the two-node beam element
κ = geometric thermal conductivity constant
λ = second Lame constant
μ = first Lame constant
ν = Poisson ratio
ξ_{ijmn} = relaxation tensor
ρ = material density
σ = stress in a standard linear solid
σ_{ij} = stress tensor
τ = characteristic relaxation time
τ_ε = time constant of relaxation of stress under constant strain
τ_σ = time constant of relaxation of strain under constant stress
ϕ_n = nth undamped mode shape vector
ψ = integration variable
ω_n = nth undamped natural frequency
$\hat{\omega}_n$ = nth damped natural frequency

Presented as Paper 2002-1729 at the AIAA/ASME/ASCE/AHS/ASC 43rd Structures, Structural Dynamics, and Materials Conference, Denver, CO, 22–25 April 2002; received 19 July 2004; revision received 14 April 2005; accepted for publication 26 May 2005.

*Graduate Research Assistant, Center for Aerospace Structures, Department of Aerospace Engineering Sciences; Mark.Silver@Colorado.edu. Student Member AIAA.

†Professor, Center for Aerospace Structures, Department of Aerospace Engineering Sciences; Lee.Peterson@Colorado.edu. Associate Fellow AIAA.

‡Senior Aerospace Engineer, Space Vehicles Directorate, 3550 Aberdeen Avenue SE; Richard.Erwin@kirtland.af.mil. Senior Member AIAA.

Introduction

LARGE space structure modeling often focuses on obtaining acceptable fidelity in the stiffness and mass of the structure. Damping is often overlooked. In large space structures, damping

can be as important as stiffness in resisting on-orbit disturbances.[1] Modeling damping can be an important element of any large space structure design.

The literature draws a distinction between interface- and material-related damping.[2] Interface damping depends most on the mechanics of the interface and the mechanics of the materials at the interface.[3] There are techniques for modeling interface damping; many of these are empirical and require component tests. In most space structures, interface damping due to deployable joints can often be the dominant source of damping.

However, recent design trends in high-precision deployable space structures have had the inadvertent design effect of all but eliminating interface dissipation. This is because the nonlinear hysteresis due to friction at the interface mechanics provides an undesirable mechanism for instability at optical wavelengths.[4,5] In fact, joints for deployable optics are being designed to reduce the interface damping to perhaps 0.1% or critical damping or less.[3,4] When the space structure must also be cryogenic, material damping may become a significant source of damping.[6]

The present study is motivated by the need to quantify material damping for the design of such high-precision spacecraft structures. Knowledge of the fundamental sources of damping existing in all solids has been around for more than 50 years.[7] Of these fundamental sources, elastothermodynamic dissipation is the most significant in metals, at least an order of magnitude larger than the other fundamental dissipative mechanisms.[2] Early work on elastothermodynamic dissipation by Zener[7] showed that including the effects of elastothermodynamic dissipation in the constitutive relationship parallels that of a standard linear viscoelastic solid in beam geometries only. Various experiments on this problem have successfully verified Zener's elastothermodynamic dissipative predictions for beams.[8,9] More recent analytical work in this area includes a general development of elastothermodynamic dissipation for any three-dimensional body by Alblas[10] and extension of Zener's work for axial interfaces within a rod by Kinra and Milligan.[11] A first step toward constructing a general theory for elastothermodynamic damping in composites was presented by Bishop and Kinra.[12,13] Givoli and Rand[14] presented the conditions under which elastothermodynamic damping becomes significant in rods. A numerical analysis of the general, three-dimensional problem was presented by Farhat et al.[15] by using temperature degrees of freedom in the finite element method (FEM) to numerically model the strain/temperature interaction. Around the same time in the finite element literature, Segalman[16] presented a method for determining explicit damping and differential stiffness matrices from a general viscoelastic constitutive relation to be included in a dynamic finite element analysis.

This present work combines the linear coupled elastothermodynamic dissipation theory of beams determined by Zener with the explicit matrix method of Segalman and presents a method for predictive modeling of elastothermodynamic material damping in beams by using FEMs without the use of temperature degrees of freedom. This allows predictions of elastothermodynamic damping in finite element models. The present finite element formulation is the first of its kind to be found in the literature. The free vibration of a solid metal beam with a rectangular cross section and a representative truss structure are used as example cases. The beam FEM results are compared with the Zener theory predictions, and the truss structure results are discussed. One interesting result of this study is that elastothermodynamic theory increases for modes with a larger component of strain energy due to bending rather than extension of the truss members.

In the first section of the paper, background on dissipative mechanisms in materials is presented. The importance of one fundamental form of dissipation in materials, elastothermodynamic damping, is discussed. Previous work on elastothermodynamic dissipation is summarized along with a brief derivation of the coupling effect between the stress, strain, and temperature relation and the heat conduction equation that results in elastothermodynamic damping. Then, the method that Zener used to simplify this coupling for the analysis of beams and rods is presented. In the second section, implementation of the elastothermodynamic damping of beams in the FEM by the method proposed by Segalman is presented. First, the Segalman method is used for assembling the damping matrices of a 12-degree-of-freedom beam element. Finite element results for beams of various materials and geometries are compared to Zener's theoretical predictions. Finally, the method is applied to a representative truss structure and the resulting damping predictions are discussed.

Dissipative Mechanisms in Materials

Damping sources within solids can be divided into three categories. The first category is damping resulting from material inhomogeneity. The second category is material viscoelasticity. The third category is damping from fundamental sources, meaning that it occurs even in a theoretical solid with no imperfections.[2]

In the first category, the term "material inhomogeneity" has a rather broad meaning, the exact definition of which varies for each material type. In composite materials, which are inherently inhomogeneous due to the fiber/matrix composition, fiber/fiber and fiber/matrix contact interactions both leading to damping.[17] In metals, the corresponding inhomogeneity can take the form of crystal-to-crystal alignment imperfections, foreign atoms within the crystal, and asymmetry in the shape of the crystal.[18] Material inhomogeneities are difficult to predict and depend highly on the formation of the material. Therefore, models of damping of inhomogeneous origin are most often the result of empirical relations.

The second category of dissipation mechanisms in materials, viscoelasticity, is caused by the deformation-rate-dependent response of the material. Damping of this kind is most pronounced in polymers and is the most significant source of damping in small-amplitude vibration in composites.[17]

The third category includes damping mechanisms considered fundamental in all solid materials. These arise from coupling between material behavior and thermodynamic principles. Two forms of fundamental damping exist in every solid: dissipation due to the coupling between heat transfer and strain rate (elastothermodynamic dissipation) and dissipation due to interactions between sound waves and thermal oscillation. A third exists only in materials with free electrons: dissipation due to interactions between electron oscillation and temperature oscillation. The elastothermodynamic dissipation is the focus of the present study.

Elastothermodynamic Dissipation

Elastothermodynamic damping is the fundamental dissipative mechanism most prominent in the elastic vibration of metals.[2] The term "elastothermodynamic damping" represents the loss in energy from an entropy increase caused by the coupling of heat transfer and the strain rate. After the initial coupling equations were published by Nowacki,[19] Zener was the first to relate this coupling to an energy loss in vibration (see Ref. 10). A thorough examination of dissipation in metals was presented by Zener[7] in 1948. In this monograph, the relations for elastothermodynamic dissipation are derived from basic energy conservation in a material along with irreversible thermodynamic theory. Zener also shows that, with certain assumptions about the geometry, the elastothermodynamic dissipation can be related to an equivalent viscoelastic material. These assumptions were used to relate elastothermodynamic dissipation to the constitutive relation that Zener called a "standard linear solid." The relation, as given by Zener, is

$$\sigma + \tau_\varepsilon \dot{\sigma} = M_R(\varepsilon + \tau_\sigma \dot{\varepsilon}) \tag{1}$$

The relaxed elastic modulus refers to the modulus M_R of a material after either of the aforementioned relaxations has taken place.

To relate elastothermodynamic dissipation to the standard linear solid equation, begin with the linear, coupled, elastothermodynamic relations. First is the linear elastothermodynamic stress/strain relation for an isotropic material, also known as the Duhamel–Neuman form of Hooke's law. In indicial notation, this equation is

$$\sigma_{ij} = \delta_{ij}\lambda\varepsilon_{kk} + 2\mu\varepsilon_{ij} - \delta_{ij}(3\lambda + 2\mu)\alpha(T - T_0) \tag{2}$$

The second equation required to define the linear, coupled, elastothermodynamic theory is the energy equation, given by

$$kT_{,mm} = \rho c_E \dot{T} + (3\lambda + 2\mu)\, T_0 \dot{\varepsilon}_{kk} \tag{3}$$

In Eq. (3) it has been assumed that the temperature differential is small enough that the varying temperature T, normally multiplied by the strain rate in this equation, can be replaced by the constant T_0. The most significant assumption made to relate these two equations to a standard linear solid is to eliminate spatial coordinates in the energy equation. Zener does this by expanding the temperature field in terms of time and spatially varying components. Here, the temperature is expanded by the equation

$$T(x_i, t) = \sum_j T_j(t) S_j(t) \tag{4}$$

These functions must satisfy a characteristic equation along with appropriate boundary conditions. The characteristic equation and boundary conditions for temperature are

$$(k/c_E\rho)(S_{i,kk}) + S_i/\tau = 0, \qquad S_i = 0 \qquad \text{at} \qquad x_i = \pm d/2 \tag{5}$$

In this case, the geometric boundary condition d is the thickness of a beam. The solutions to this equation show that the temperature varies periodically through the thickness of the beam. This assumption also implies that the temperature varies in only one direction; in this case it varies along the thickness. This changes the relation of stress and temperature from a three-dimensional temperature change, $3\lambda + 2\mu$, to that of a single dimension, $2\mu(1-\nu)$. Use of Eq. (5) requires that the thermal conductivity k in Eq. (3) be replaced by a constant, κ, related to the geometric boundary conditions, resulting in

$$\kappa T = \rho c_E \dot{T} + [2\mu(1-\nu)] T_0 \dot{\varepsilon}_{kk} \tag{6}$$

Here the geometry-related constant for a beam of thickness d in transverse bending is

$$\kappa = k\pi^2/d^2 \tag{7}$$

In the constitutive relation of Eq. (2), there is no thermal coupling for the case $i \neq j$. That is, elastothermodynamic dissipation occurs only in deformations causing volumetric change.

Solving for the temperature in Eq. (2), substituting in Eq. (6) for T and the first derivative of T, and then solving for stress gives the energy equation in stress, strain, and their first derivatives:

$$\sigma_{ij} = \lambda\varepsilon_{kk} + 2\mu\varepsilon_{ij} + \Big((\rho c_E/\kappa)\dot{\sigma}_{ij} - (2\mu\rho c_E/\kappa)\dot{\varepsilon}_{ij} - \dot{\varepsilon}_{kk} \times \left\{\rho c_E \lambda/\kappa + [\alpha 2\mu(1-\nu)]^2 T_0/\kappa\right\}\Big) \tag{8}$$

The first two terms on the right-hand side of Eq. (8) make up the isotropic linear elastic relation. The third bracketed term contains the damping effect, similar to a viscosity, from elastothermodynamic dissipative sources. This damping term will be used in conjunction with a method presented by Segalman[16] to define the damping and dissipative stiffness in the FEM. Before presenting this method, current methods of incorporating damping in many commercial finite element packages will be discussed.

Implimentation of Damping in the FEM

Overview of Current Commercially Available Techniques

The most common techniques used for implementing damping in commercial finite element codes require a priori knowledge of damping as an intrinsic property.[20] Rayleigh damping defines the damping matrix as a linear combination of the stiffness and mass matrix. Modal damping uses a value for each material that is a fraction of critical damping associated to that material. This critical damping fraction is converted into an average for each mode weighted by the mass matrix. The structural damping method determines damping forces that are opposed to the velocity vectors within the structure from the forces caused by stressing the structure. This kind of damping is applicable only when the displacement and velocity are out of phase by 90 deg. Critical damping factors can be used to define damping in each eigenmode as a fraction of the critical damping for that mode. All of the previous methods require some empirical evidence of the damping to be implemented correctly.

Some methods for applying damping do not require a priori knowledge of the actual structural damping. In some analyses dashpot elements can be used to define discrete damping.[20] However, these dashpot elements work only in defined directions, and using them in two- or three-dimensional models can be overly complicated. Another method involves bulk viscosity, or damping associated with volumetric straining. The bulk viscosity method creates a pressure that is linear or quadratic in the volumetric strain rate. It is also called truncation frequency damping.[20] This form of damping is generally used only to damp the numerical problems stemming from the highest element frequencies or to eliminate numerical problems during high-speed dynamics.

Viscoelastic materials can be used in most commercial finite element codes. Viscoelastic material definitions are normally taken from creep or relaxation test data for a material. Although this technique does not require a priori knowledge of the dynamic response of the structure, its use in dynamic modeling is constrained to steady-state dynamics.[21]

Differential Stiffness and Damping Matrices for Viscoelastic Structures

The damping method presented by Segalman[16] uses a linear viscoelastic material relation to define damping and additive stiffness matrices in the FEM. These additional matrices are defined in the following general second-order equation of motion:

$$M\ddot{x} + \Delta C\dot{x} + [K^e + \Delta K^t(t)]x = Q(t) \tag{9}$$

Here, the total viscoelastic stiffness matrix is broken up into a constant elastic part, K^e, and a small time-varying part. In this method, the two terms that are defined to include the damping effect are the time-varying small viscoelastic stiffness matrix, ΔK^t, and the damping matrix, ΔC. First, the only time-varying component, ΔK^t, is converted to the frequency domain by a Fourier transform, namely,

$$\Delta K^*(\omega_n) = \int_0^\infty i\omega_n \Delta K^t(\psi) e^{-i\omega_n\psi} d\psi \tag{10}$$

In the finite element equations, the differential stiffness matrix is created by the relation

$$\Delta K = \mathrm{Re}\left[\sum_n \Delta K^*(\omega_n)\phi_n(z_n)^T\right] \tag{11}$$

where the dual vector z_n is defined as

$$z_n = \frac{K^e\phi_n}{(\phi_n)^T K^e \phi_n} \tag{12}$$

Because the ΔK is assembled with the vector multiplication of the undamped mode shape vector and the dual vector, the resulting matrix is nonsymmetric and nonsparse. This can lead to computational feasibility problems when this matrix is stored for even moderately sized models.

The damping matrix is created in the same fashion, except that it uses the imaginary part of the frequency domain small viscoelastic component:

$$\Delta C = \sum_n \mathrm{Im}\left[\frac{1}{\omega_n}\Delta K^*(\omega_n)\phi_n(z_n)^T\right] \tag{13}$$

As with the ΔK matrix, here the resulting ΔC matrix is nonsymmetric and nonsparse, leading to computational feasibility problems.

By using these relations for the damping and differential stiffness matrix, the linear coupled elastothermodynamic theory can now be applied. The elastothermodynamic finite element equation of motion becomes

$$M\ddot{x} + \Delta C\dot{x} + (K^e + \Delta K)x = Q(t) \tag{14}$$

Application to Linear Elastothermodynamic Model

Elastothermodynamic Relation

From the energy equation in terms of stress and strain given in Eq. (8), a time-varying solution can be found. The Laplace transform of Eq. (8), assuming a zero stress/strain initial state, gives

$$\hat{\sigma}_{ij}(s) = \lambda\hat{\varepsilon}_{kk}(s) + 2\mu\hat{\varepsilon}_{ij}(s) + \Big((\rho c_E s/\kappa)[\hat{\sigma}_{ij}(s) - 2\mu\hat{\varepsilon}_{ij}(s) - \hat{\varepsilon}_{kk}(s)] - \hat{\varepsilon}_{kk}(s)\big\{sT_0[\alpha 2\mu(1-\nu)]^2/\kappa\big\}\Big) \tag{15}$$

Then define

$$\hat{\sigma}_{ij}(s) = H(s) + 2\mu\hat{\varepsilon}_{ij}(s) - \hat{\varepsilon}_{kk}(s) \tag{16}$$

Substitute Eq. (16) into Eq. (15) and solve for $H(s)$, yielding

$$H(s) = s\hat{\varepsilon}_{kk}(s)\left(\frac{1}{s - \kappa/\rho c_E}\right)\frac{T_0[\alpha 2\mu(1-\nu)]^2}{\rho c_E} \tag{17}$$

Placing Eq. (17) into Eq. (16) and taking the inverse Laplace transform yields

$$\sigma_{ij} = \lambda\varepsilon_{kk} + 2\mu\varepsilon_{ij} + \int_0^t \left\{\frac{T_0[\alpha 2\mu(1-\nu)]^2}{\rho c_E} \times e^{\kappa\psi/\rho c_E}\dot{\varepsilon}_{kk}(t-\psi)\right\}d\psi \tag{18}$$

Here, as in Eq. (8), the first two terms of the right-hand side make up the isotropic linear elastic relation. The third term is the elastothermodynamic component resulting from the thermal coupling, which, as was presented previously, can be represented by a viscoelastic material model in the case of beams. However, unlike the viscoelastic material case, in this equation the third, temperature-dependent, term is represented by a convolution integral.

Implementation in Segalman Method

As presented previously, the damping method presented by Segalman is a discretization technique for linearly viscoelastic structures. For the small viscoelasticity case, the finite element stiffness matrix is assembled in the following equation, where the elastic part of the stiffness equation is separated from the small viscoelastic part as in Eq. (9):

$$K(\psi) = K^e + \int_\Omega V_{ijmn}(\psi, X)\, B_{ij}^T(X) B_{mn}(X) dX \tag{19}$$

Here, the strain-displacement matrix B_{ij} relates the generalized displacements to the strain at particle X, in body Ω.

Remark: The small viscoelastic relaxation tensor from Eq. (19) is similar to the general definition of the stress response of a linear viscoelastic structure, stated in Eq. (20) for reference[16]:

$$\sigma_{ij}(t, X) = \int_0^t \xi_{ijmn}(\psi, X)\dot{\varepsilon}_{mn}[(t-\psi), X]\, d\psi \tag{20}$$

For the case of elastothermodynamic dissipation in beams, the equivalent small relaxation tensor is written as

$$V_{ijmn} = \frac{T_0[\alpha 2\mu(1-\nu)]^2}{\rho c_E} e^{(\kappa/\rho c_E)\tau} \tag{21}$$

The equation for the frequency domain component of the stiffness matrix [Eq. (8) from the description of the Segalman method] becomes Eq. (22). From here, assembly of the damping and differential stiffness matrix is straightforward.

The FEM analyses used a 12-degree-of-freedom beam implemented in a MATLAB®-based research finite element code. Both the transverse and extensional damping characteristics are included in the formulation. Beams of various fundamental frequencies were modeled in the FEM. The results were compared to the corresponding analytical theory Zener named "the vibration of reeds." The symmetric, elemental $\Delta\tilde{K}^*$ matrix for a 12-degree-of-freedom, Bernoulli–Euler beam is

$$\Delta\tilde{K}^*(\omega_n) = \int_0^\infty \int_\Omega [B_{ij}(X)]^T \left\{ i\omega_n \frac{T_0[\alpha 2\mu(1-\nu)]^2}{\rho c_E} \times e^{(\kappa/\rho c_E - i\omega_n)\psi}\right\} B_{mn}(X) dX\, d\psi \tag{22}$$

which, written in matrix form, becomes

$$\Delta\tilde{K}^* = L^3 \times \begin{bmatrix}
L^2AD_L & 0 & 0 & 0 & 0 & 0 & -L^2AD_L & 0 & 0 & 0 & 0 & 0 \\
0 & 12I_zD_{Ty} & 0 & 0 & 0 & 6LI_zD_{Ty} & 0 & -12I_zD_{Ty} & 0 & 0 & 0 & 6LI_zD_{Ty} \\
0 & 0 & 12I_yD_{Tz} & 0 & -6LI_yD_{Tz} & 0 & 0 & 0 & -12I_yD_{Tz} & 0 & -6LI_yD_{Tz} & 0 \\
0 & 0 & 0 & 0 & 0 & 0 & 0 & 0 & 0 & 0 & 0 & 0 \\
0 & 0 & -6LI_yD_{Tz} & 0 & 4L^2I_yD_{Tz} & 0 & 0 & 0 & 6LI_yD_{Tz} & 0 & 2L^2I_yD_{Tz} & 0 \\
0 & 6LI_zD_{Ty} & 0 & 0 & 0 & 4L^2I_zD_{Ty} & 0 & -6LI_zD_{Ty} & 0 & 0 & 0 & 2L^2I_zD_{Ty} \\
-L^2AD_L & 0 & 0 & 0 & 0 & 0 & L^2AD_L & 0 & 0 & 0 & 0 & 0 \\
0 & -12I_zD_{Ty} & 0 & 0 & 0 & -6LI_zD_{Ty} & 0 & 12I_zD_{Ty} & 0 & 0 & 0 & -6LI_zD_{Ty} \\
0 & 0 & -12I_yD_{Tz} & 0 & 6LI_yD_{Tz} & 0 & 0 & 0 & 12I_yD_{Tz} & 0 & 6LI_yD_{Tz} & 0 \\
0 & 0 & 0 & 0 & 0 & 0 & 0 & 0 & 0 & 0 & 0 & 0 \\
0 & 0 & -6LI_yD_{Tz} & 0 & 2L^2I_yD_{Tz} & 0 & 0 & 0 & 6LI_yD_{Tz} & 0 & 4L^2I_yD_{Tz} & 0 \\
0 & 6LI_zD_{Ty} & 0 & 0 & 0 & 2L^2I_zD_{Ty} & 0 & -6LI_zD_{Ty} & 0 & 0 & 0 & 4L^2I_zD_{Ty}
\end{bmatrix} \tag{23}$$

where the damping terms are

$$D_L = \frac{LT_0\omega_n E^2\alpha^2}{\left(c_E L^2 E\rho\omega_n - ik\right)}, \qquad D_{T_y} = \frac{T_0\omega_n E^2\alpha^2}{(i\kappa_y + c_E\rho\omega_n)}$$

$$D_{T_z} = \frac{T_0\omega_n E^2\alpha^2}{(i\kappa_z + c_E\rho\omega_n)} \tag{24}$$

The degrees of freedom are ordered as

$$[u_{x1} \quad u_{y1} \quad u_{z1} \quad \theta_{x1} \quad \theta_{y1} \quad \theta_{z1} \quad u_{x2} \quad u_{y2} \quad u_{z2} \quad \theta_{x2} \quad \theta_{y2} \quad \theta_{z2}] \tag{25}$$

In Eq. (23), the x direction is along the length of the beam. Therefore, I_y and I_z are the second moments of inertia of the beam cross section in the y and z directions, respectively. In Eq. (24), κ_y and κ_z refer to the geometry-dependent thermal conductivity terms, defined for transverse deflection of a beam in Eq. (7), in the y and z directions, respectively.

Finite Element Verification: Elastothermodynamic Dissipation in an Aluminum Beam

According to the Zener theory for the free vibration of a beam, vibration closest to the frequency of maximum elastothermodynamic dissipation, also known as the elastothermodynamic relaxation frequency, should show the most dissipation from elastothermodynamic coupling. Tests have been completed to verify Zener's predictions for the damping of beams (see Refs. 8 and 9). The tests were completed in such a way as to minimize other sources of damping. Different test specimens were designed to have first natural frequencies ranging above and below the elastothermodynamic relaxation frequency.

In the FEM, the critical damping fraction values ζ were taken from the state-space model built from the mass, damping, and stiffness matrices. These were compared to the values calculated by using Zener's method. A plot of the log of the ratio of the vibration frequency to Zener's predicted elastothermodynamic relaxation frequency vs the log of ζ is shown in Fig. 1. Besides showing the accuracy of the finite element implementation, Fig. 1 also shows a key result from the Zener theory; namely, that matching the first natural frequency of a free beam with the elastothermodynamic relaxation frequency creates the maximum amount of damping. Here note that when the first natural frequency was lower than the elastothermodynamic relaxation frequency [i.e., $\log(\omega_1 \cdot \tau) < 0$], vibration at higher mode numbers closer to the elastothermodynamic relaxation frequency contained more critical damping than the first mode.

Each beam model consisted of 25 Bernoulli–Euler beam elements and used the same cross-section geometry, whereas the length was varied in each analysis to change the first natural frequency. Each beam element contained six degrees of freedom per node, making a total of 156 degrees of freedom per model. The modeling technique converged to within 1% variation in ζ with only three elements in the beam. With six or more elements per beam, the numerical variation in ζ has converged to less than 0.6%.

Finite Element Investigation: Elastothermodynamic Dissipation in an Aluminum Truss

A more complex model of a truss was built to test the code and gain more insight into the implications of the analysis method for design. An eight-bay truss with a square cross section was meshed by using 500 aluminum beam elements. Each longeron, batten, and diagonal is meshed with five elements. One end of the truss is supported rigidly, and the opposite end has four lumped mass elements. In each model considered, the cross sections of each longeron, batten, and diagonal were all square with identical widths. A diagram of the model is shown in Fig. 2.

One of the questions to be considered with this model was how elastothermodynamic damping could be enhanced by design. A key part of this question concerns the role of local truss member bending

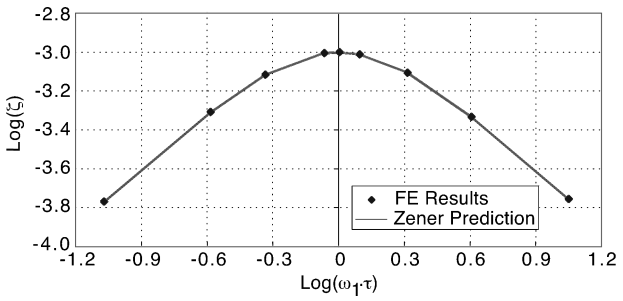

Fig. 1 Critical damping fraction vs ratio of ω_1 to Zener frequency for a free vibrating aluminum beam.

Table 1 Truss model parameters

Model	Tip mass, kg	Square beam dimension, mm	Peak member damping frequency, Hz
A	80	5	3.07
B	8	5	3.07
C	160	5	3.07
D	80	1	76.7
E	80	1.6	29.9
F	80	10	0.767

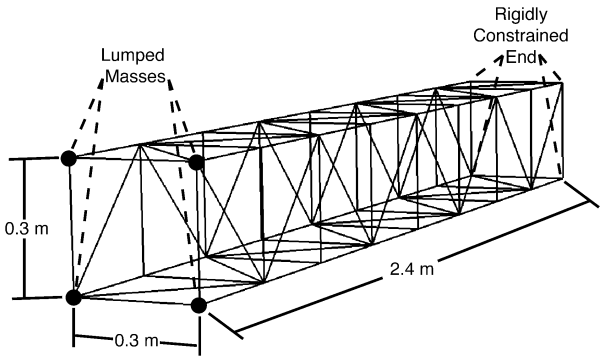

Fig. 2 Truss finite element model.

in determining a particular mode's damping ratio. One would expect from the preceding theoretical development that elastothermodynamic damping in beam extensional vibration should be much lower than in transverse vibration. This is because the thermodynamic transport distance is the beam thickness for transverse vibration, but it is the truss member length for longitudinal vibration. Thus, unless the beam truss members have very small length-to-radius-of-gyration ratios, elastothermodynamic damping would be higher in transverse vibration of the truss elements. Additionally, as was seen in the investigation of the free vibration of a beam, matching the vibration frequency with the peak elastothermodynamic damping frequency (the so-called Zener frequency) also increased the amount of damping. Therefore, the key for maximizing the elastothermodynamic damping seem to be synchronizing the member and damping frequencies and optimizing the mode shape to include transverse member vibration.

For each model, an energy analysis was used to quantify the amount of "local bending" in a particular mode shape. Because all of the elements of this model are beams, the amount of strain energy in bending, torsion, and extension can be separated out explicitly. In this case, the global stiffness matrix can be written as

$$K^e = EI\left(\bar{K}^e_{EI}\right) + GJ\left(\bar{K}^e_{GJ}\right) + EA\left(\bar{K}^e_{EA}\right) \tag{26}$$

where each of the $\bar{K}^e$ terms correspond to the stiffness due to bending, torsion, and extension. The total strain energy in a given mode shape is then given by

$$\begin{aligned} U^n &= \phi_n^T K^e \phi_n \\ &= \phi_n^T EI\left(\bar{K}^e_{EI}\right)\phi_n + \phi_n^T GJ\left(\bar{K}^e_{GJ}\right)\phi_n + \phi_n^T EA\left(\bar{K}^e_{EA}\right)\phi_n \\ &= U^n_{EI} + U^n_{GJ} + U^n_{EA} \end{aligned} \tag{27}$$

in which $U^n_{()}$ are the modal strain energy due to bending, torsion, and extension. The fraction of strain energy in a mode due to bending of the truss members is then given by

$$\eta^n = U^n_{EI} \big/ U^n \tag{28}$$

As an initial investigation into designing a truss to maximize elastothermodynamic damping, a truss configuration was chosen such that the Zener frequency of the members is close to the first few natural frequencies of vibration of the truss. This specific design is labeled as model A in Table 1. The computed modal frequencies and damping ratios for this model are listed in Table 2.

Table 2 Frequency, damping, and bending energy results for trusses with varying tip mass

Model	Tip mass, kg	Section, mm	Mode number	Frequency, Hz	ζ	Bending energy, %
A	80	5	1	3.16	6.10*e*–7	6.17*e*–2
			2	3.23	5.20*e*–7	5.26*e*–2
			3	4.19	6.21*e*–4	65.9
			4	12.8	3.74*e*–7	8.37*e*–2
			5	30.7	3.00*e*–7	0.154
			6	53.0	7.48*e*–7	0.655
			7	55.2	9.12*e*–7	0.834
			8	56.9	7.52*e*–6	7.08
			9	93.4	5.84*e*–5	90.1
			10	94.8	5.83*e*–5	91.2
			11	97.6	5.74*e*–5	92.6
			12	99.1	5.88*e*–5	96.2
			13	99.4	5.85*e*–5	96.0
			14	101	5.75*e*–5	96.3
B	8	5	1	9.67	4.31*e*–7	7.58*e*–2
			2	9.89	3.81*e*–7	6.81*e*–2
			3	12.9	2.94*e*–4	66.4
			4	39.3	3.11*e*–7	0.203
			5	90.9	6.42*e*–6	9.65
			6	93.4	5.84*e*–5	90.1
			7	94.8	5.83*e*–5	91.3
			8	97.6	5.74*e*–5	92.6
			9	98.6	2.94*e*–5	48.4
			10	99.1	5.86*e*–5	95.8
			11	99.3	5.77*e*–5	94.8
			12	101	4.59*e*–5	76.8
			13	102	5.42*e*–5	94.1
			14	102	5.59*e*–5	90.8
C	120	5	1	2.24	5.80*e*–7	6.16*e*–2
			2	2.29	4.98*e*–7	5.25*e*–2
			3	2.96	6.51*e*–4	65.8
			4	9.10	4.95*e*–7	8.28*e*–2
			5	21.8	3.71*e*–7	0.136
			6	38.2	2.80*e*–7	0.178
			7	40.0	3.25*e*–7	0.216
			8	41.4	8.89*e*–6	6.11
			9	86.9	3.79*e*–7	0.545
			10	86.9	4.12*e*–7	0.592
			11	87.0	1.70*e*–7	0.244
			12	87.5	1.81*e*–7	0.266
			13	93.4	5.83*e*–5	90.1
			14	94.8	5.82*e*–5	91.2

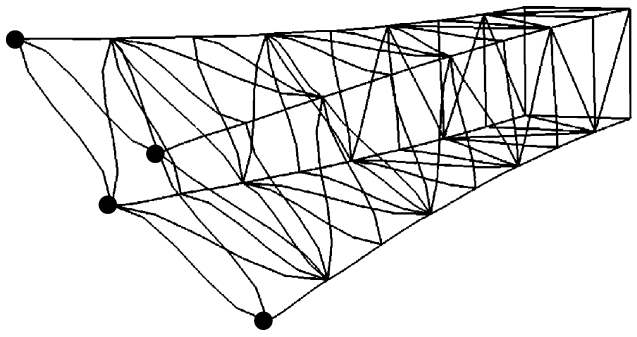

Fig. 3 Deformed baseline model; $\omega_3 = 4.19$ Hz, $\zeta_3 = 6.21e{-}4$.

One might expect that this model would exhibit higher damping in the modes with frequency close to the Zener frequency. However, the larger damping values tended to correspond to mode shapes that contain a relatively large amount of member bending. In Table 2, the mode numbers for model A with the larger damping ratios are 3, 8, and 9–14. Modes 3 and 8 are dominated by shearing of the truss cross section. The bending of the members in mode 3 can be seen in the mode shape plot of Fig. 3. Likewise, modes 9–14 are all local deformation modes involving significant bending of the truss members.

As a further investigation into the correlation between member bending and elastothermodynamic damping, a total of six different combinations of cross-section widths and tip masses were modeled. The parameters for each model are listed in Table 1.

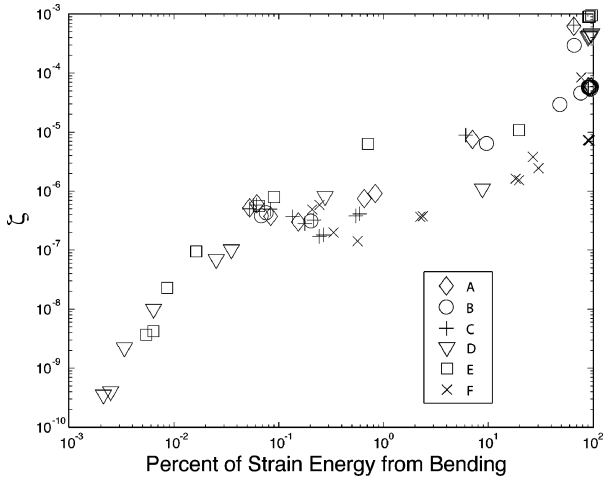

Fig. 4 Critical damping fraction vs percent bending energy for all models.

The percent of strain energy due to bending in the first 14 modes of each model resulting from the energy analysis are listed in Tables 2 and 3. Additionally, the critical damping fraction vs percent bending strain energy is plotted in Fig. 4. Here it is clearly shown that modes involving a relatively high percentage of strain energy from bending exhibit the largest amount of elastothermodynamic damping.

Returning to the design space mentioned at the beginning of this section, a model was created with truss member cross sections

Table 3 Frequency, damping, and bending energy results for trusses with varying cross-section geometry

Model	Tip mass, kg	Section, mm	Mode number	Frequency, Hz	ζ	Bending energy, %
D	80	1	1	0.48	1.10*e*–6	8.82
			2	0.63	4.04*e*–10	2.48*e*–3
			3	0.65	3.55*e*–10	2.11*e*–3
			4	2.58	2.23*e*–9	3.36*e*–3
			5	6.16	1.01*e*–8	6.36*e*–3
			6	11.0	7.00*e*–8	2.52*e*–2
			7	11.5	1.02*e*–7	3.52*e*–2
			8	11.7	8.15*e*–7	2.77*e*–1
			9	18.7	4.10*e*–4	90.2
			10	18.9	4.21*e*–4	91.3
			11	19.5	4.38*e*–4	92.7
			12	19.8	4.62*e*–4	96.3
			13	19.9	4.62*e*–4	96.1
			14	20.3	4.73*e*–4	96.7
E	80	1.6	1	0.82	1.07*e*–5	19.7
			2	1.01	4.24*e*–9	6.34*e*–3
			3	1.04	3.70*e*–9	5.41*e*–3
			4	4.12	2.30*e*–8	8.59*e*–3
			5	9.86	9.55*e*–8	1.63*e*–2
			6	17.5	5.59*e*–7	6.48*e*–2
			7	18.4	7.93*e*–7	8.99*e*–2
			8	18.6	6.31*e*–6	0.711
			9	29.9	8.91*e*–4	90.2
			10	30.3	9.02*e*–4	91.3
			11	31.2	9.15*e*–4	92.7
			12	31.7	9.50*e*–4	96.3
			13	31.8	9.48*e*–4	96.1
			14	32.5	9.52*e*–4	96.7
F	80	10	1	6.26	5.84*e*–7	0.245
			2	6.39	4.87*e*–7	0.208
			3	13.9	8.44*e*–5	77.5
			4	25.4	1.99*e*–7	0.334
			5	60.5	1.42*e*–7	0.566*e*
			6	92.7	3.67*e*–7	2.25
			7	95.9	3.76*e*–7	2.38
			8	107	3.79*e*–6	26.8
			9	171	1.63*e*–6	18.3
			10	187	7.31*e*–6	89.9
			11	188	2.45*e*–6	30.3
			12	189	7.29*e*–6	91.1
			13	195	7.19*e*–6	92.5
			14	196	1.53*e*–6	19.7

designed to have a Zener frequency equal to that of the local modal frequencies of the truss. This configuration should maximize the amount of damping from the two design variables. This model is labeled as model E in Table 1. This model did indeed generate the largest amount of elastothermodynamic damping of all of the models considered. For the higher frequency local modes, it had an average of 14 times more damping than the model with the next highest damping magnitudes for modes 9–14. This result shows that both mode shape and member Zener frequency should be considered in designing a structure for optimum elastothermodynamic damping. The methods presented in this paper allow a designer to combine these two previously separate analyses into a single coupled model.

Conclusions

This paper presented a method that allows the assembly of damping and additive stiffness matrices for elastothermodynamic damping in beam finite elements, as would be used for large space truss structures. A technique proposed by Zener[7] is used to relate elastothermodynamic damping in beams to a viscoelastic constitutive relation. The result from Zener's technique is then used in the method of Segalman[16] for general viscoelastic constitutive relations to build the finite element matrices for the case of elastothermodynamic damping in beams. The results show that the damping found in the FEM accurately matches Zener's damping prediction for beams. Various configurations of a hypothetical full-scale truss were modeled to show the significance of global damping predictions from this method. Results from the truss analyses show that a critical source of elastothermodynamic damping in the truss comes from local member bending. A truss configuration was presented that maximized the amount of damping both from matching the member natural frequencies to the Zener frequency and from matching the member natural frequencies to that of the higher frequency local modes of the truss. This example demonstrates the unique ability of the code to allow a designer to combine the two coupled effects into a single model. Future work should consider imposing a sparsity constraint on the assembled damping matrices to enable the formulation of large-scale models.

Acknowledgments

Part of this research was completed while the first author was at the U.S. Air Force Research Laboratory in the Space Scholars summer program in 2001 (http://spacescholars.plk.af.mil/). R. Scott Erwin was the research mentor for this program.

References

[1]Peterson, L. D., and Hinkle, J. D., "Implications of Structural Design Requirements for Selection of Future Space Telescope Architectures" *Proceedings of the SPIE Annual Meeting*, SPIE-5166-05, Society of Photo-Optical Instrumentation Engineers (International Society for Optical Engineering), Bellingham, WA, 2003.

[2]Braginsky, V. B., Mitrofanov, V. P., and Panov, V. I., *Systems with Small Dissipation*, translated by Erast Gliner, Univ. of Chicago Press, Chicago, 1985.

[3]Lake, M. S., and Hachkowski, M. R., "Design of Mechanisms for Deployable, Optical Instruments: Guidelines for Reducing Hysteresis," NASA TM-2000-210089, March 2000.

[4]Hardaway, L. M. R., and Peterson, L. D., "Nanometer Scale Spontaneous Vibrations in a Deployable Truss Under Mechanical Loading," *AIAA Journal*, Vol. 40, No. 10, 2002, pp. 2070–2076.

[5]Peterson, L. D., and Hinkle, J. D., "Microdynamic Design Requirements for Large Space Structures," AIAA Paper 2003-1451, April 2003.

[6]Peng, C. Y., Leland, R., Levine, M., and Shido, L., "Experimental Observations on Material Damping at Cryogenic Temperatures," SPIE Annual Meeting, SPIE-5528A-7, Society of Photo-Optical Instrumentation Engineers (International Society for Optical Engineering), Bellingham, WA, 2004.

[7]Zener, C., *Elasticity and Anelasticity of Metals*, Univ. of Chicago Press, Chicago, 1948.

[8]Crawley, E. F., and van Schoor, M. C., "Material Damping in Aluminum and Metal Matrix Composites," *Journal of Composite Materials*, Vol. 21, June 1987, pp. 533–568.

[9]Bishop, J. E., and Kinra, V. K., "Some Improvements in the Flexural Damping Measurement Technique," *M3D: Mechanics and Mechanisms of Material Damping*, American Society for Testing and Materials, Philadelphia, 1992, pp. 457–470.

[10]Alblas, J. B., "A Note on the Theory of Elastothermodynamic Damping," *Journal of Thermal Stresses*, Vol. 4, July–Oct. 1981, pp. 333–355.

[11]Kinra, V. K., and Milligan, K. B., "Irreversible Heat Transfer as a Source of Thermoelastic Damping," *M3D: Mechanics and Mechanisms of Material Damping*, American Society for Testing and Materials, Philadelphia, 1992, pp. 94–123.

[12]Bishop, J. E., and Kinra, V. K., "Thermoelastic Damping of a Laminated Beam in Flexure and Extension," *Journal of Reinforced Plastics and Composites*, Vol. 12, Feb. 1993, pp. 210–226.

[13]Bishop, J. E., and Kinra, V. K., "Elastothermodynamic Damping in Laminated Composites," *International Journal of Solids and Structures*, Vol. 34, No. 9, 1997, pp. 1075–1092.

[14]Givoli, D., and Rand, O., "Dynamic Thermoelastic Coupling Effects in a Rod," *AIAA Journal*, Vol. 33, No. 4, 1995, pp. 776–778.

[15]Farhat, C., Park, K. C., and Dubois-Pelerin, Y., "An Unconditionally Stable Staggered Algorithm for Transient Finite Element Analysis of Coupled Thermoelastic Problems," *Computer Methods in Applied Mechanics and Engineering*, Vol. 85, No. 3, 1991, pp. 349–365.

[16]Segalman, D. J., "Calculation of Damping Matrices for Linearly Viscoelastic Structures," *Journal of Applied Mechanics*, Vol. 54, Sept. 1987, pp. 585–588.

[17]Hwang, S. J., and Gibson, R. F., "The Use of Strain Energy-Based Finite Element Techniques in the Analysis of Various Aspects of Damping of Composite Materials and Structures," *Journal of Composite Materials*, Vol. 26, No. 17, 1992, pp. 582–605.

[18]Nowick, A. S., and Berry, B. S., *Anelastic Relaxation in Crystalline Solids*, Academic Press, New York, 1972.

[19]Nowacki, W., *Thermoelasticity*, Addison Wesley, Reading, MA, 1962.

[20]*ABAQUS Theory Manual*, Hibbitt, Karlsson and Sorensen, Inc., Pawtucket, RI, 2000.

[21]Morman, K. N., and Nagtegaal, J. C., "Finite Element Analysis of Sinusoidal Small-Amplitude Vibrations in Deformed Viscoelastic Solids. Part I: Theoretical Development," *International Journal of Numerical Methods in Engineering*, Vol. 19, No. 7, 1983, pp. 1079–1103.

B. Balachandran
Associate Editor